

General Disclaimer

One or more of the Following Statements may affect this Document

- This document has been reproduced from the best copy furnished by the organizational source. It is being released in the interest of making available as much information as possible.
- This document may contain data, which exceeds the sheet parameters. It was furnished in this condition by the organizational source and is the best copy available.
- This document may contain tone-on-tone or color graphs, charts and/or pictures, which have been reproduced in black and white.
- This document is paginated as submitted by the original source.
- Portions of this document are not fully legible due to the historical nature of some of the material. However, it is the best reproduction available from the original submission.

DRL 126
DRD Se 8

DOE/JPL-955567-82/6
Distribution Category UC-63

9950-668

TRIENNIAL REPORT

on the

DESIGN, ANALYSIS, AND TEST VERIFICATION
OF ADVANCED ENCAPSULATION SYSTEMS

For Period Ending

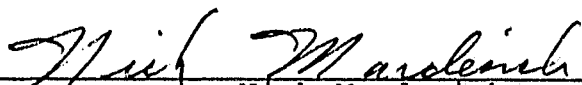
30 November 1981

Contract 955567

Prepared by:

Alec Garcia
Chuck Minning

Approved by:



Nick Mardesich
Group Manager
Product Development
Advanced Programs

SPECTROLAB, INC.
12500 Gladstone Avenue
Sylmar, California 91342

March 1982

The JPL Flat-Plate Solar Array Project is sponsored by the U.S. Department of Energy and forms part of the Solar Photovoltaic Conversion Program to initiate a major effort toward the development of low-cost solar arrays. This work was performed for the Jet Propulsion Laboratory, California Institute of Technology by agreement between NASA and DOE.

N82-26782

Unclas
23509

CSCI 10A G3/44

(NASA-CR-169048) DESIGN, ANALYSIS, AND TEST
VERIFICATION OF ADVANCED ENCAPSULATION
SYSTEMS Triennial Report, period ending 30
Nov. 1981 (Spectrolab, Inc.) 23 P
HC A02/HF A01



This report was prepared as an account of work sponsored by the United States Government. Neither the United States nor the United States Department of Energy, nor any of their employees, nor any of their contractors, subcontractors, or their employees, makes any warranty, express or implied, or assumes any legal liability or responsibility for the accuracy, completeness or usefulness of any information, apparatus, product or process disclosed, or represents that its use would not infringe privately owned rights.

ORIGINAL PAGE IS
OF POOR QUALITY

TABLE OF CONTENTS

<u>Section</u>	<u>Title</u>	<u>Page</u>
1.0	SUMMARY STATEMENT	1
2.0	INTRODUCTION	2
3.0	TECHNICAL DISCUSSION	3
3.1	Thermal Testing	3
3.2	Thermal/Structural Tests	10
3.3	Structural/Deflection Test	15
3.4	Electrical Test	17
3.5	Optical Test Results	17
4.0	CONCLUSIONS AND RECOMMENDATIONS	20
5.0	PLANNED ACTIVITIES	21

Section 1.0
SUMMARY STATEMENT

All verification testing was completed during this period. Preliminary results and observations are discussed. Descriptions of the thermal, thermal structural, and structural deflection test setups are included. Detailed reporting of all verification testing will be contained in the Periodic Report Supplement concerning Phase II testing.

Section 2.0

INTRODUCTION

The objective of this program is to develop analytical methodology for advanced encapsulation designs. From these methods design sensitivities will be established for the development of photovoltaic module criteria and the definition of needed research tasks.

The program consists of three phases. In Phase I, analytical models were developed to perform optical, thermal, electrical, and structural analyses on candidate encapsulation systems. From these analyses several candidate systems will be selected for qualification testing during Phase II. Additionally, during Phase II, test specimens of various types will be constructed and tested to determine the validity of the analysis methodology developed in Phase I. In Phase III, a finalized optimum design based on knowledge gained in Phases I and II will be developed and delivered to JPL.

Section 3.0

TECHNICAL DISCUSSION

3.1 THERMAL TESTING

The module/panel fixture was designed to permit the radiative boundary (air, ground) to be predominantly determined by the front and back panels which are low iron glass and a high emissivity black panel, respectively. The glass permits 91% of the short wavelength flux to be transmitted (at rated voltage) while it is essentially opaque to low temperature infrared radiation. Off rated-voltage-operation shifts the source spectrum to slightly longer wavelengths.

For the present test, the circulating air is used to maintain a steady air temperature beneath the thermal modules. It is not used to create a forced convective flow past the modules. Rather, the flow related heat transfer mechanism should be that of natural convection. The module/panel fixture design is flexible enough to allow greater as well as smaller spacing and repositioning of the thermal test modules.

Repositioning or other changes of the module/panels alters the radiative environment. To allow for these contingencies, the RENO computer program is used to determine script-F radiative interchange factors. Perspective plots of the chamber and module/panels are shown in Figures 1 through 3. These were generated using the SPLOT program, a preprocessor for the RENO

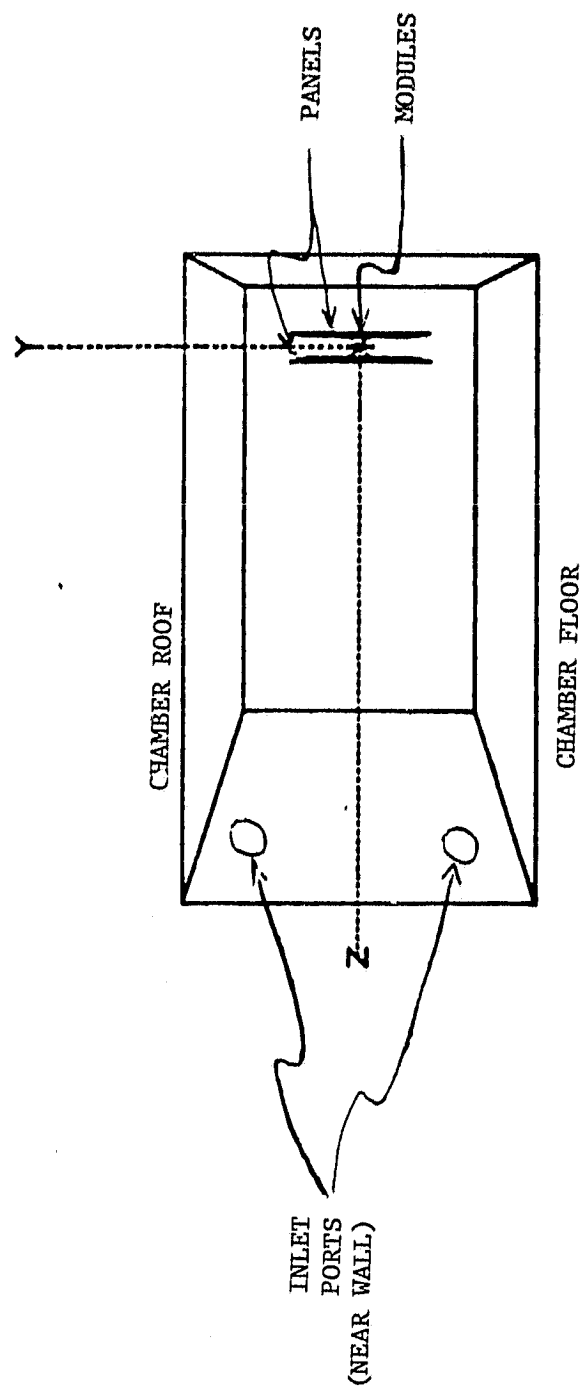


Figure 1. SIDE VIEW OF BALLEY CHAMBER, WITH PANELS, MODULES AND INLET PORTS SHOWN

EXHAUST SLOT
ABOVE MODULES

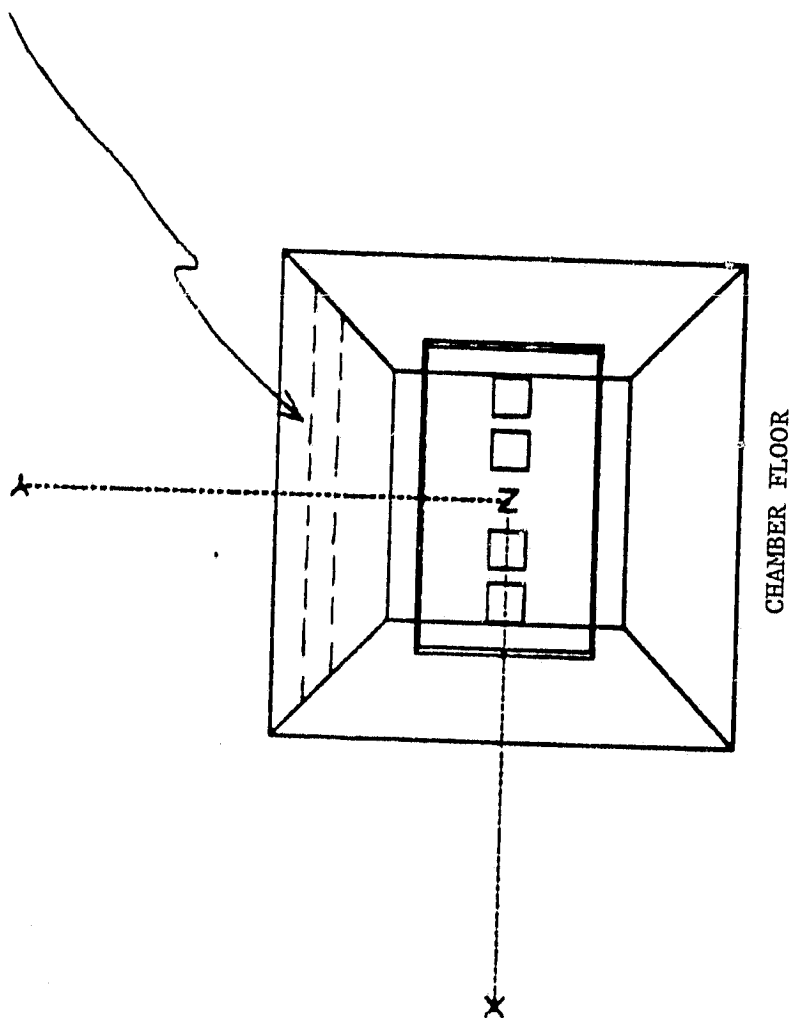


Figure 2. BACK VIEW OF BAILEY CHAMBER WITH PANELS, MODULES AND EXHAUST SLOT SHOWN

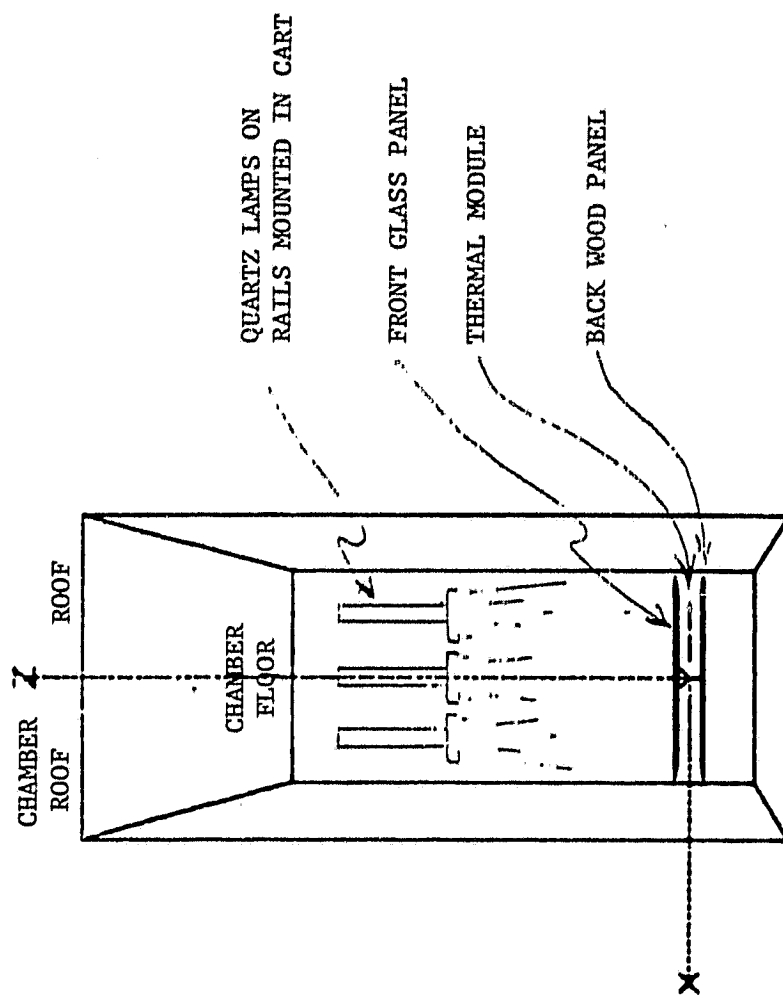


Figure 3. TOP VIEW OF BALLEY CHAMBER WITH SOURCES, MODULES AND FRONT AND BACK PANELS IN PLACE

Program, and show the relative position of the various components used in the test. The surfaces are treated as gray surfaces with the chamber walls having an emissivity of .09. As is apparent from the side or top view (Figure 1 and 3), the closer the modules and panels the more dominant is the module/panel interchange. As the separation increases, other surfaces participate more significantly in the interchange. The separation is 4" in Figures 1 through 3. The chamber length and width are 14' and 7' respectively.

Figures 2 and 3 show the circulating air inlet ports and exhaust slot. A maximum of 810 cfm is available with port obstruction and bleed ports providing flow rate control. The exhaust slot draws off the stratified hotter air near the roof of the chamber. At steady state the temperature difference between exhaust and input is proportional to the power input to the chamber via the quartz lamps.

Three lamp fixtures are mounted on rails which in turn are attached to a cart. This allows repositioning of the lamps with respect to the thermal modules. The source module separation distance is the primary means of controlling source intensity at the modules. Intensity uniformity, separation and power input (number of bulbs) are varied to result in a uniform specified flux with as little disturbance of air at and beneath the thermal module. The input voltage of the 1000 watt quartz lamps is 140 volts. The equal energy intervals are thus based on the average of spectral energy at 500W and 1500W at a particular wavelength.

The values are shown in Figures 4 and 5. The resulting data is used to determine the midpoint wavelength of each energy interval. Lower lamp voltages can be taken into account by assuming the source spectrum to be that of a black body at the corresponding

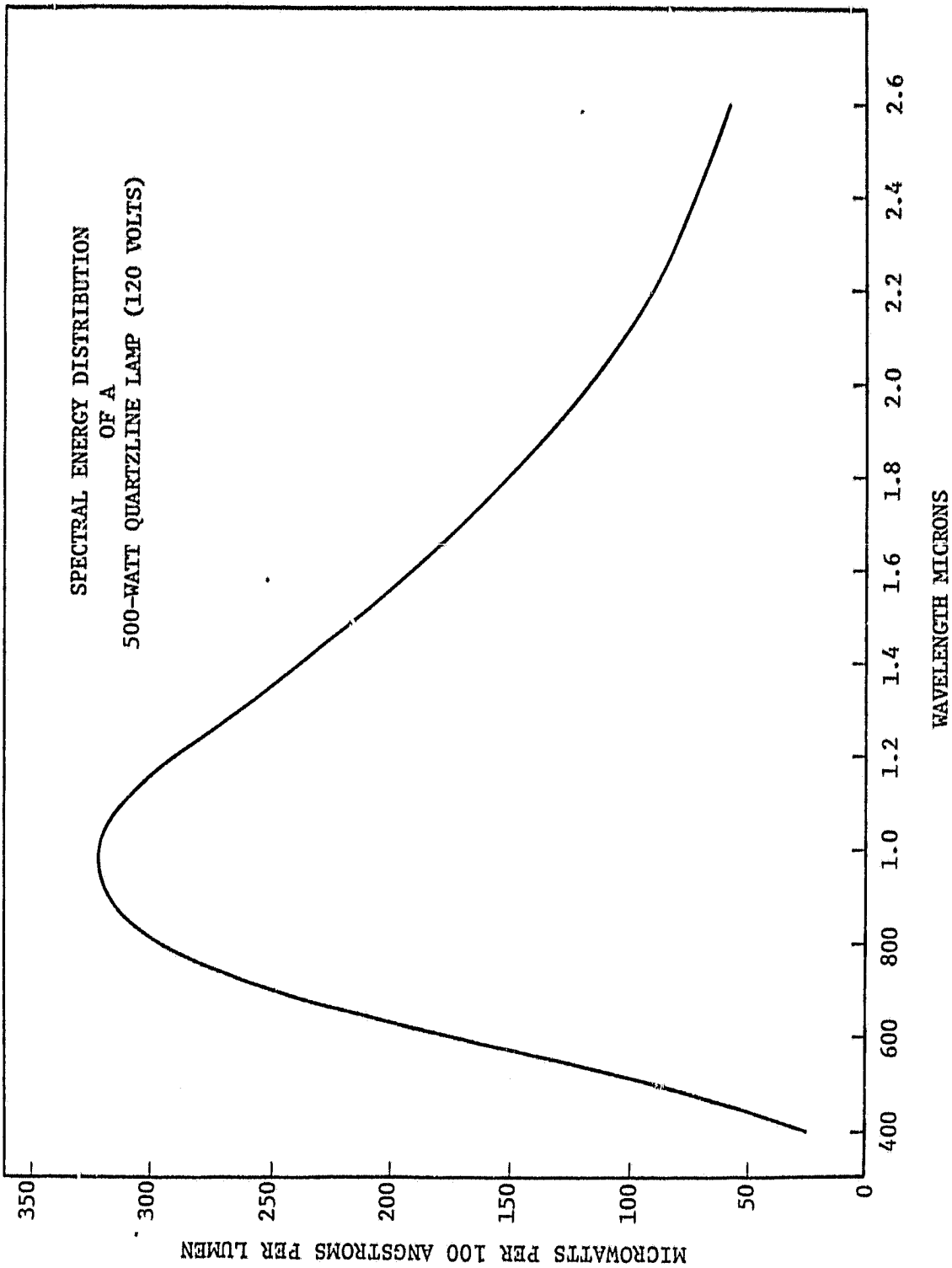


Figure 4. QUARTZ SPECTRUM FOR 500 WATT BULB

ORIGINAL PAGE IS
OF POOR QUALITY

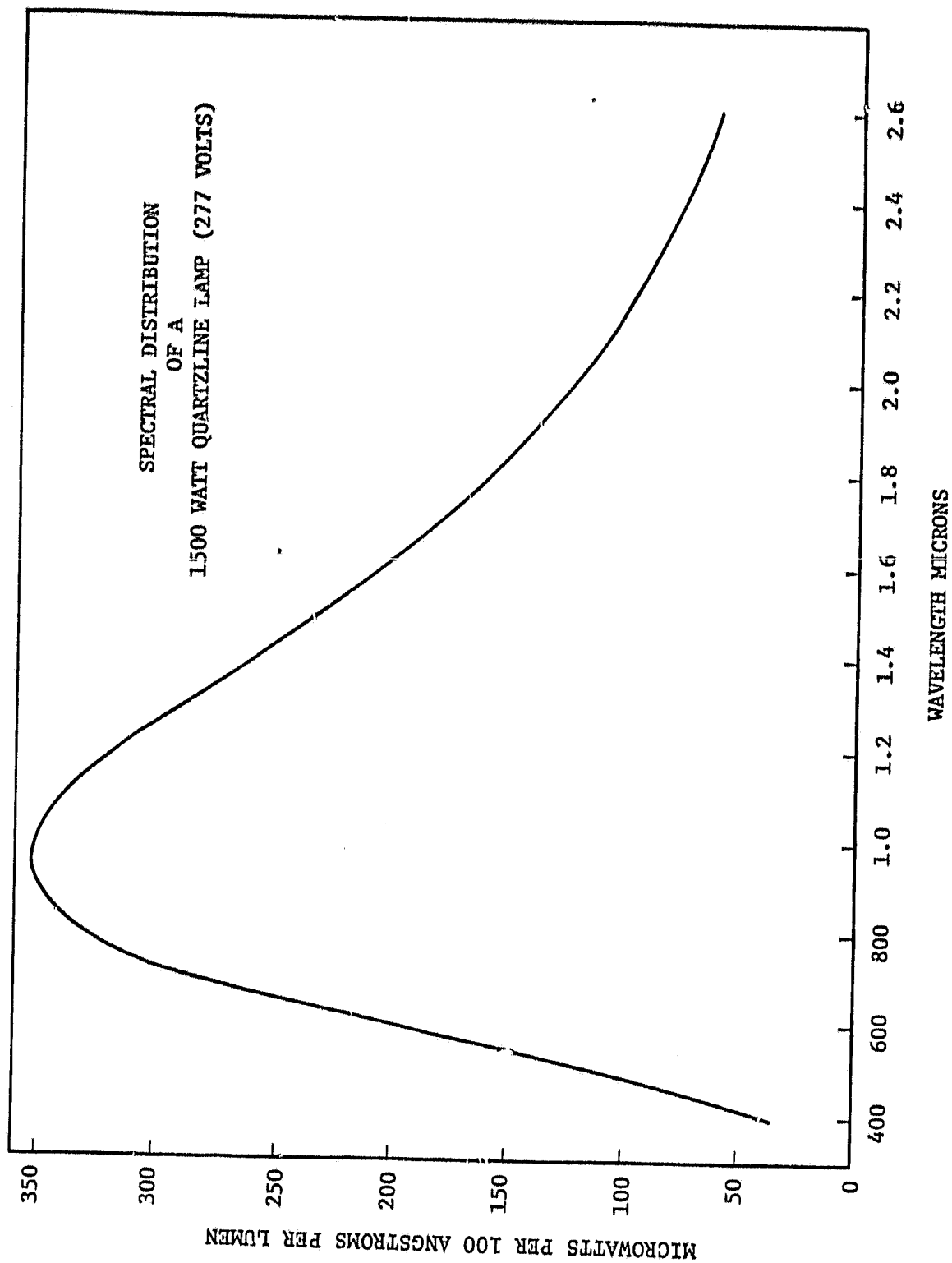


Figure 5. QUARTZ SPECTRUM FOR 500 WATT BULB

filament temperature. The curves are normalized such that the integrated value equals the intensity measured by the flux measurement devices to be described.

Both a HyCal pyrheliometer and a Spectrolab SR-75 are used to measure intensity and uniformity over the thermal modules. The latter is retained to provide setpoints prior to each test. The initial measurements will be taken with the front glass panel in place.

Estimates of module and glass panel response times are based on the thermal capacitance and natural convection coefficient for these components. The module response time is about 1/2 hour. The glass response time is approximately 1/3 hour. The absorption in the front glass panel was estimated through the use of the optical program. This is accomplished by setting $N_2 = N_c = 1$, $C\lambda = 0$ and $a_2 = 0$. The glass transmittance curve (Figure 6) is relatively flat over the quartz lamp source spectrum (Figures 4 and 5). Thus equal energy intervals emanating from the lamp remain equal on passage through the glass. Results of the computation indicate that 91% of the energy is transmitted, 7% reflected and 2% absorbed for a 1/8" glass thickness. These estimates do not take into account the line-source like behavior which would occur if the lamps are close to the glass front panel. This can result in preferential heating of the glass and can be modeled (RENO computer program) by assuming the front glass panel consists of three isothermal sections.

3.2 THERMAL/STRUCTURAL TESTS

The thermal/structural test was completed during this period. Some preliminary conclusions/results are:

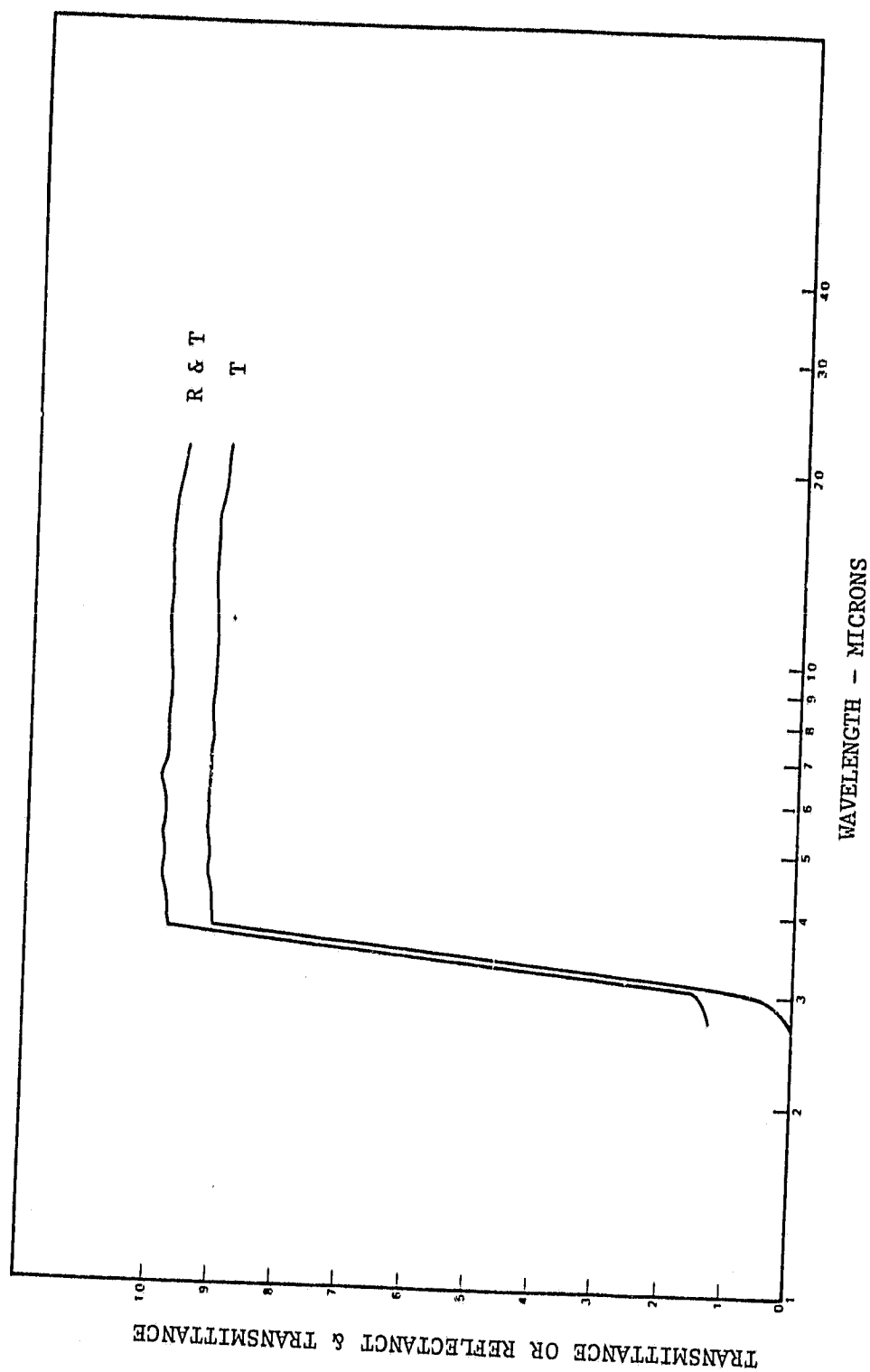


Figure 6. TRANSMITTANCE AND TRANSMITTANCE PLUS REFLECTANCE VERSUS WAVELENGTH FOR NO-IRON GLASS

1. No cell or substrate damage occurred as a result of the tests.
2. The mechanical strains due to mismatch of thermal expansions of the test coupon materials are small compared to the "apparent" strains. The "apparent" strain is caused by (1) thermal mismatch between the strain gage and the material to which it is bonded, and (2) by a change in resistance of the strain gage as the temperature changes. Both of these effects are non-linear with respect to temperature.

The test coupon strain measurements include both the actual mechanical strain and the apparent strains. "Apparent" strain measurements were made for each combination of strain gage and substrate material, and for the strain gage/silicon cell combination at each temperature data point. The actual mechanical strains in the cells and substrates are determined by subtracting the "apparent" strains from the test coupon strain measurements. The mechanical strains are then compared to the analytical predictions in order to validate the analytical models.

Table 1 shows the specimens tested. This table, showing the actual pottant thickness as measured is a revision of an earlier table showing nominal thicknesses. A typical specimen is shown in Figure 7.

These specimens were subjected to the following temperature-step sequences:

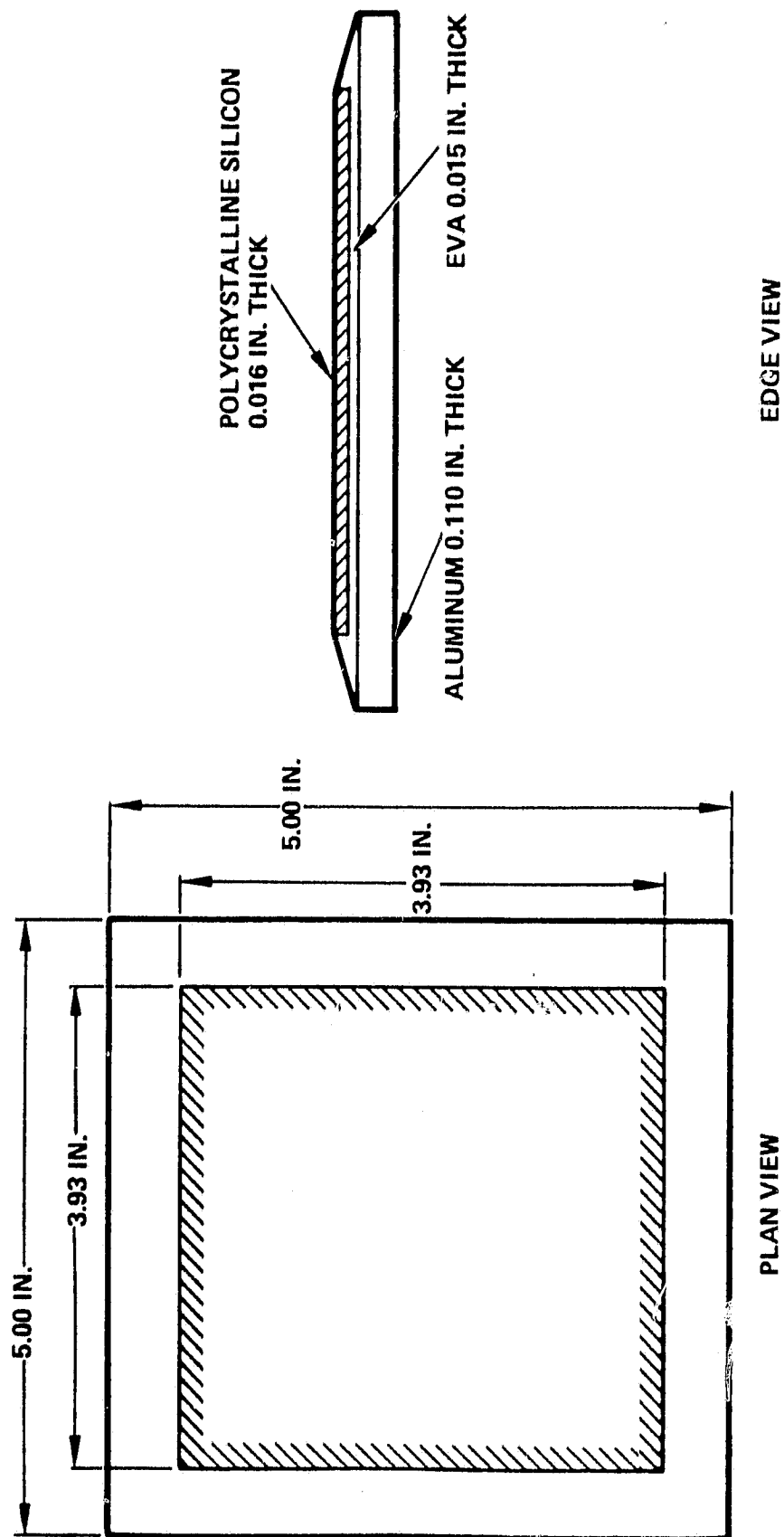
Specimen	
TSC-1, 2, 3 and -6, 7, 8, 9, 10	Ambient → 40 → 60 → 80 → 100 → 80 → 60 → 40 → 20 → 0 → -20 → -40 → -20 → 0 → 20 → Ambient

Table 1
THERMAL/STRUCTURAL VERIFICATION TEST SPECIMENS

COUPON NO.	TSC-1	TSC-2	TSC-3	TSC-4	TSC-5	TSC-6	TSC-7	TDC-8	TSC-9	TSC-10	TSC-11	TSC-12
Load Bearing Member	Low Iron Glass	Low Iron Glass	Low Iron Glass	Low Iron Glass	Low Iron Glass	Al	Al	Mil Stl	Mil Stl	Mil Stl	Mil Stl	Mil Stl
Top Cover	-	-	-	-	-	Tedlar	Tedlar	Tedlar	Tedlar	Tedlar	Tedlar	Tedlar
Encapsulant	EVA	Sili-cone	Sili-cone	Urethane	Urethane	EVA	Sili-cone	EVA	Sili-cone	Sili-cone	Urethane	Urethane
Encapsulant Thickness, mil	16.0	5.5	11.5	4.5	16.0	7.5	19.0	5.0	11.0	11.0	11.0	15.0
Cell Type	PC-4" Sq	PC-4" Sq	PC-4" Sq	PC-4" Sq	PC-4" Sq	PC-4" Sq	PC-4" Sq	PC-4" Sq	PC-4" Sq	PC-4" Sq	PC-4" Sq	PC-4" Sq
No. Cells*	1	1	1	1	1	1	1	1	1	1	1	1

*Etched silicon wafers will be used in place of finished cells.

Figure 7. TEST COUPON DIMENSIONS: THERMAL/STRUCTURAL TEST



TSC-4, 5, 11, 12

Ambient → 40 → 60 → 80 → 100
→ 80 → 60 → 40 → 20 → 0
→ 20 → Ambient

Specimens TSC-4, 5, 11 and 12 were subjected to the narrower temperature range because the glass transition temperature of the poxtant (polyurethane) used in these specimens is -10°C . To avoid overstressing the cells (by subjecting these specimens to temperatures $< -10^{\circ}\text{C}$) and risking possible damage to the specimen before completion of the regular test sequence, the minimum temperature was restricted to 0°C .

Overstress tests were performed on specimens TSC-1, 2, and 3.

The temperature-step sequence was: Ambient → 20 → 0 → -20
→ -40 → -60 → -40 → -20 → 0 → 20 → 40 → 60 → 80 → 100 → 120 → 140
→ 120 → 140 → 120 → 100 → 80 → 60 → 40 → Ambient.

A steady-state period of at least 1/2 hour was attained for each temperature in the sequence.

3.3 STRUCTURAL/DEFLECTION TEST

The structural/deflection tests were completed. The test panels were loaded at 10 PSF increments up to 50 PSF for the qualification test and to 100 PSF for the overstress tests. Some preliminary results and observations are:

1. Measured center-of-panel deflections at 50 PSF loading ranged from about 0.4 inch for the ribbed wood and steel substrate panels, 0.6 inch for the glass superstrate panels, and 1.4 inches for the unribbed wood substrate panels.
2. The measured deflections indicate good correlation with the analytical predictions.

ORIGINAL PAGE IS
OF POOR QUALITY

3. No cell breakage occurred as a result of the deflection tests.
4. With the exception of 2 ribbed wood panels, no load bearing layers failed at pressures up to 100 PSF (overstress).
5. Three ribbed wood panel configurations were tested. These were:
 - a. Uniform ribs with the ends of the ribs unsupported by the test fixture.
 - b. Uniform ribs with the ends of the ribs supported by the test fixture.
 - c. Tapered ribs with the ends unsupported by the test fixture.

Configuration a and c failed at 30 PSF loading due to delamination of the wood panels at the ends of the ribs. The bonds between the ribs and the panels remained intact. Configuration b, however, sustained 50 PSF loading without failure and the deflection closely matched the analytical predictions. The important difference between configuration b and configuration a and c is that in configuration b the rib loads were carried directly to the support fixture, consistent with the analytical model. In configurations a and c however, the rib loads had to pass through the panels before reaching the support fixture. The concentration of load and the stiffness discontinuity at the ends of the ribs exceeded the flatwise tension capability of the panels in the thickness direction.

6. Some of the encapsulant layers had substantial void content.
7. Some cells were broken prior to testing.

ORIGINAL PAGE IS
OF POOR QUALITY

The test data will be analyzed in order to compare the measured strains with the analytical predictions.

The structural/deflection test fixture was fabricated from a surplus steel trash container. A four-foot square test specimen rests on four steel angle bars bolted to the inside periphery of the container, as shown in Figure 8. A uniform pressure load is applied to the specimen by filling the upper portion (i.e., above the specimen) of the test fixture with water. The water is contained within a large plastic bag. The entire fixture is pivoted on one edge, and a load cell is used to determine the amount of water in the test fixture. The weight of the water is directly proportional to the pressure load on the module.

3.4 ELECTRICAL TEST

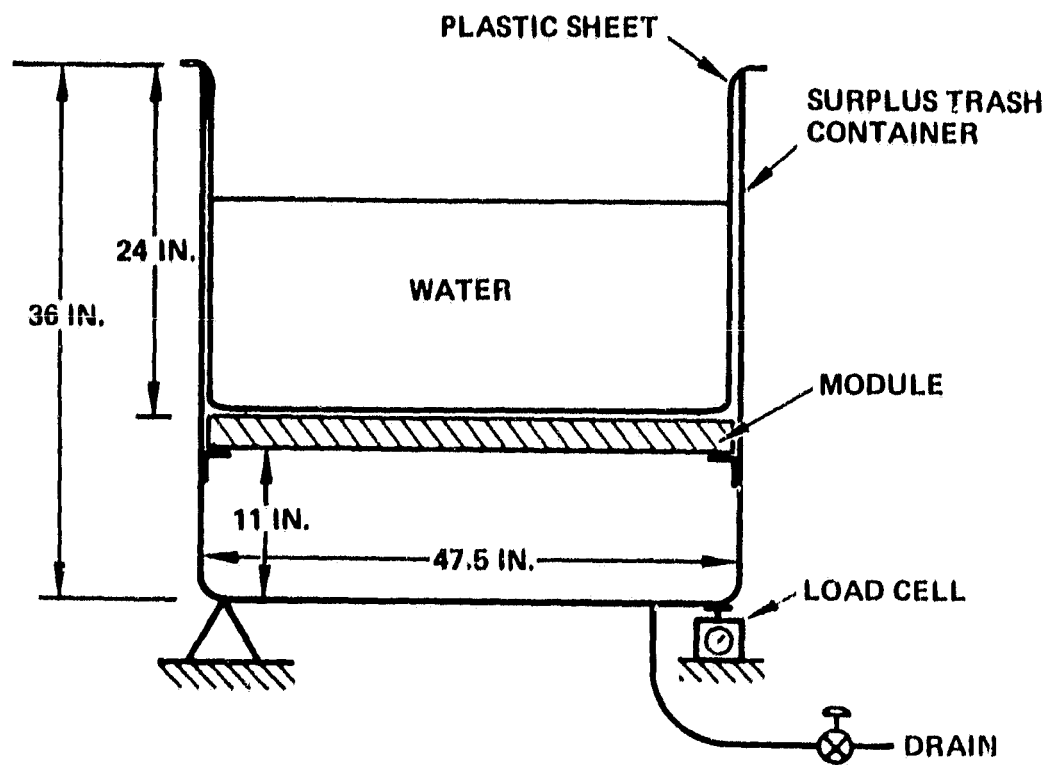
Predicted values of maximum and minimum voltage at electrical breakdown are compared against experimentally measured values in Table 2. The voltage predictions were computed using the values of dielectric strength and dielectric constant listed in Appendix A of the Phase One Topical Report. These predictions also do not account for flaws such as cracks, pinholes, and bubbles that may have been present in the test samples.

3.5 OPTICAL TEST RESULTS

The results of the optical tests have not yet been completely analyzed. A full report will be included in the Phase II Test Report.

ORIGINAL PAGE 1
OF POOR QUALITY

Figure 8. STRUCTURAL/DEFLECTION TEST
TEST FIXTURE DETAILS



MAXIMUM ΔP ACROSS MODULE = 125 PSF

ORIGINAL PAGE IS
OF POOR QUALITY

Table 2

COMPARISON OF PREDICTED AND MEASURED VALUES OF V_0 AT BREAKDOWN

SPECIMEN TYPE	SIDE	DESCRIPTION	V ₀ BREAKDOWN, kV			
			Measured		Predicted	
			Max.	Min.	Max.	Min.
A	Front	.004" Tedlar/.018" EVA CG	19	12	14	11.84
B	Front	.001" Tedlar/.018" EVA CG	19	12	11.43	11.33
C	Front	.001" Tedlar/.018" EVA	21	5	11.43	11.33
D	Front	.001" Tedlar/.036" EVA CG	22	10	22.59	22.49
D*	Front	.001" Tedlar/.036" EVA CG	25	12	22.59	22.49
A	Back	.018" EVA/CG, .001" Al Polyester	11	1	11.16	11.16
B	Back	.036" EVA/CG, .001" Al Polyester	13	5	22.32	22.32
C	Back	.018" EVA/CG, .125" Wood	25	8	24.3	23.9
D	Back	.036" EVA/CG, .125" Wood	25	21	26.78	26.01

Section 4.0

CONCLUSIONS AND RECOMMENDATIONS

There are no conclusions and recommendations for this period.

Section 5.0
PLANNED ACTIVITIES

During the next period analysis of Phase II verification testing will be completed. Construction will begin on qualification module after JPL approval of designs.